Comunicações Geológicas, 2004, t. 91, pp. 99-116

Petrology of Spinel Peridotite Xenoliths from Santo Antão, Cape Verde Islands

M. H. MENDES*; R. CALDEIRA*; L. C. SILVA* & J. MUNHÁ**

Key-words: Peridotite xenoliths; upper mantle; metasomatism; Santo Antão; Cape Verde Islands.

Abstract: Ultramafic xenoliths included in Santo Antão Island nephelinitic/alkali basaltic lavas (Cape Verde) comprise dunite/wehrlite and harzburgite suites; the harzburgite suite shows complex textural/mineralogical features and are more refractory (Fo = 90-92) than the dunite/wehrlite suite (Fo = 82-88).

Dunite and wehrlite xenoliths are mainly spinel-bearing olivine cumulates with intercumulus clinopyroxene. Mineral chemistry and geothermometric data suggest that dunite/wehrlite xenoliths crystallized at ~ 1000 °C from Santo Antão alkalic magmas and accumulated in magma reservoirs located at depth beneath the island.

The harzburgite xenoliths are composed of olivine + orthopyroxene + spinel ± clinopyroxene. According to textural and mineralogical relations, harzburgite xenoliths were divided into three groups: I – protogranular, II – metasomatized protogranular and III – porphyroclastic. The complex thermal evolution recorded by these xenoliths – high fO_2 values ($\Delta FMQ = 0.7 - 1.9$) and development of abundant CO_2-rich fluid inclusions, are attributed to recent infiltration of harzburgites by melts trapped/crystallized within the mantle. These features and the refractory nature of the harzburgite suite support the interpretation that these xenoliths represent depleted oceanic lithosphere, variously modified by magmatism associated with the genesis of Santo Antão Island.

Palavras-chave: Xenólitos peridotíticos; manto superior; metassomatismo; Santo Antão; Cabo Verde.

Resumo: Os xenólitos ultramáficos, existentes em lavas basálticas alcalinas/nefeliníticas da Ilha de Santo Antão (Cabo Verde), incluem uma série harzburgítica e uma série dunítica/wehrlítica; a série harzburgítica apresenta características texturais/mineralógicas complexas e é mais refractária (Fo = 90-92) do que a série dos dunitos/wehrlitos (Fo = 82-88).

Os xenólitos duníticos e wehrlíticos são, essencialmente, acumulados de olivina e espinela, com clinopiroxena intercumulus. A química mineral e os dados geotermométricos sugerem que os xenólitos duníticos/wehrlíticos cristalizaram a ~ 1000 °C a partir de magmas alcalinos e acumularam em câmaras magmáticas profundas, sob a ilha de Santo Antão.

Os xenólitos harzburgíticos são constituídos por olivina + ortopiroxena + espinela ± clinopiroxena. De acordo com as relações texturais e mineralógicas, os xenólitos harzburgíticos foram divididos em 3 grupos: I – protogranular, II – protogranular metassomatizado e III – porfiroclástico. A evolução térmica complexa registada nestes xenólitos, os elevados valores de fO_2 ($\Delta FMQ = 0.7 - 1.9$) e o desenvolvimento de abundantes inclusões fluidas ricas em CO_2 são atribuídos à infiltração recente nos harzburgitos de *melts*, aprisionados/cristalizados no interior do manto; estas características e a natureza refractária da série harzburgítica, apoiam a interpretação de que estes xenólitos representam litosfera oceânica empobrecida, modificada pelo magmatismo associado à génese da Ilha de Santo Antão.

INTRODUCTION

The Cape Verde archipelago comprises ten within-plate/hotspot related islands. It is located about 500 km west off the African coast and 2000 km east off the Mid Atlantic Ridge (Fig. 1). Undersaturated alkaline rocks are dominant, reflecting long-term intense magmatism that was active from upper Oligocene in Sal Island to present times (1995) in Fogo Island (Chã das Caldeiras).

Xenoliths entrained in alkali basalts frequently correspond to mantle samples carried up to the earth's surface by the ascending magma during volcanic eruptions. Thus, they are an important source of information about lithospheric composition and thermal evolution in mantle regions associated with alkaline volcanism (MENZIES, 1987).

Ultramafic xenoliths are common in Cape Verde volcanic rocks (particularly, in olivine nephelinites and olivine basalts) and were previously reported on

* Instituto de Investigacão Científica Tropical, Centro de Geologia. Alameda D. Afonso Henriques, 41 – 4D, 1000-123 Lisboa, Portugal. e-mail: cgeol@iict.pt or cgeol@clix.pt

** Departamento/Centro de Geologia, Faculdade de Ciências, Universidade Lisboa. Campo Grande Ed. C2, 1749-016 Lisboa, Portugal.

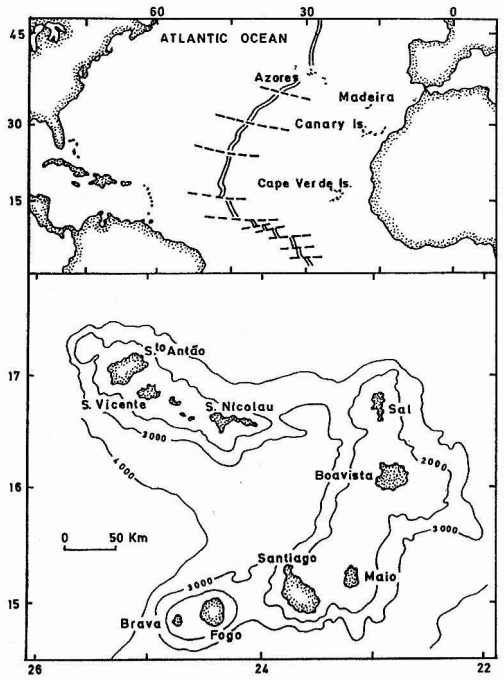

Fig. 1 – Location maps of the Cape Verde Islands (adapted from GERLACH *et al.*, 1988).

several islands (S. Nicolau – MENDES, 1984; Santiago – MENDES & SILVA, 1983; DAVIES & MENDES, 1991; MENDES, 1995; Sal – DE PAEPE & KLERKX, 1971; KOGARKO & SENIN, 1993; RYABCHIKOV *et al.*, 1995; Fogo – MUNHÁ *et al.*, 1997). These authors identified upper mantle fragments which were interpreted as metasomatized mantle residues and crystal segregations from percolating magma within the lithosphere, suggesting an heterogeneous mantle under the studied islands.

During systematic geological mapping of Santo Antão, (team of geologists from the Tropical Research Institute – IICT, the Department of Geology, University of Lisbon and the Department of Geosciences, Education Institute – ISE of Cape Verde) carried out since 1991, large (subrounded to angular, up to 20 cm in diameter) spinel peridotite xenoliths were found in nephelinitic and alkaline basaltic lavas (Pl. I, photo 1) at various locations within the Island (Fig. 2).

Peridotite samples were collected: a) in olivine melanephelinite lavas cropping out along a road section from Cova to Porto Novo and at João de Arado; b) in olivine melabasalt lavas on a road section from Ribeira Grande to Ponta do Sol; c) in melilite/perovskite-bearing

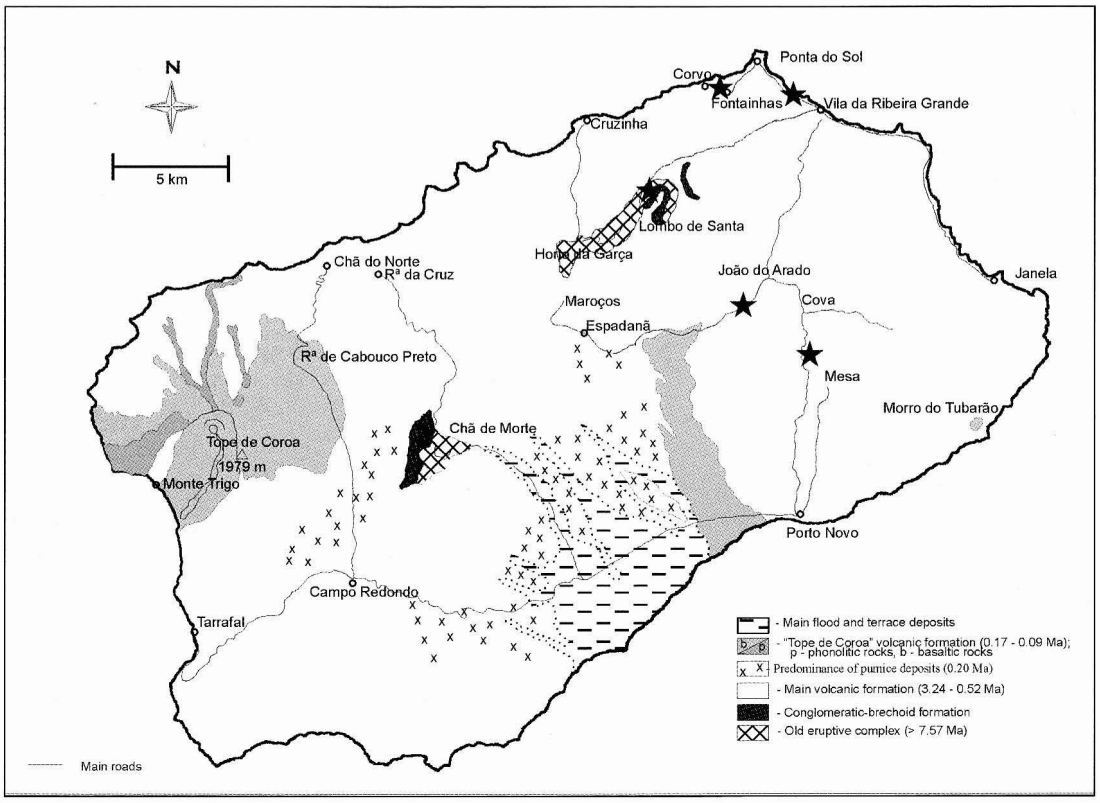

Fig. 2 – Sketch geological map of Santo Antão (after SILVA *et al.*, in preparation) with sampling locations (*stars*) of the peridotite xenoliths. Ages inferred from PLESNER *et al.* (2002).

nephelinitic lavas close to the locality of Lombo de Santa and; d) in an olivine melabasaltic dike (crosscutting basaltic lavas) at Fontainhas.

In this paper, xenoliths from Santo Antão Island are described for the first time in a contribution to characterize the lithosphere under the Cape Verde archipelago and unravel some of the complexities of the upper mantle evolution in this region. This study includes petrographic, textural, mineralogical and chemical data on peridotite xenoliths and derived temperatures of equilibrium, providing a better understanding of the magmatic processes and the nature of oceanic lithosphere beneath Santo Antão Island.

PETROGRAPHY

Modal compositions allowed classification of the studied xenoliths, following the IUGS recommendations (STRECKEISEN, 1976), into harzburgites (40-90 % Ol; 5-60 % Opx; 0-5 % Cpx), wehrlites (40-90 % Ol; 5-60 % Cpx; 0-5 % Opx) and subordinate dunites (>90 % Ol; <10 % Opx; <10 % Cpx).

Harzburgites

The harzburgite suite xenoliths have protogranular to porphyroclastic textures (MERCIER & NICOLAS, 1975; HARTE, 1977).

On the basis of their textural and mineralogical features, harzburgites were subdivided into three distinct groups:

I – Protogranular Harzburgites

Protogranular harzburgites comprise olivine and light brown enstatite together with minor amounts of pale green Cr-diopside and spinel (Pl. I, photo 2), which also constitute vermicular clusters associated with olivine and orthopyroxene.

Olivine (≤ 14 mm long) and orthopyroxene (≤ 5 mm) are subhedral to anhedral crystals and display varying degrees of development of deformation lamellae and undulose extinction. Orthopyroxene often contains exsolution lamellae of clinopyroxene and spinel. Clinopyroxene is anhedral and usually finer-grained (≤ 1 mm) than orthopyroxene and olivine. Spinel usually occurs interstitially as subhedral to vermicular grains (brown to reddish brown) and as small inclusions in the silicate minerals.

II – Metasomatized Protogranular Harzburgites

Major mineral components (olivine + orthopyroxene) are similar to those in group I protogranular harzburgites.

Characteristic metasomatic activity is evidenced by the development of abundant CO_2-rich fluid inclusions (including liquid + gaseous CO_2 and, sporadically, minute spinel crystals) and by the occurrence of K-rich silicious melt pockets within orthopyroxene (now materialised by colourless glass: SiO_2 = 64.68, TiO_2 = 1.62, Al_2O_3 = 18.34, FeO^t = 1.00, MnO = 0.02, MgO = 0.52, CaO = 0.11, Na_2O = 1.94, K_2O = 3.49 wt%) containing small neoblasts of olivine, clinopyroxene and Ti, Cr-rich spinel (Pl. I, photo 3) which is similar to anhedral dark brown spinels filling intergranular spaces between olivine and orthopyroxene. In some of these xenoliths, orthopyroxene has reacted intensely with metasomatic fluids/melts, being reduced to a few relicts that have been largely replaced by pale green Na-rich clinopyroxene (Pl. I, photo 4) which, in a number of samples, seems to corrode olivine (Pl. II, photo 1).

III – Porphyroclastic Harzburgites

Porphyroclastic harzburgites (Pl. II, photo 2) consist of olivine (2 to 3 mm) and orthopyroxene (1.5 to 2.5 mm) porphyroclasts set in a fine-grained (mainly) mylonitic matrix, including olivine and orthopyroxene neoblasts (≤ 0.3 mm) that are compositionally similar to porphyroclasts. Clinopyroxene neoblasts are rare. Spinel occurs as aggregates of small brown grains, resulting from fragmentation of larger crystals, and as minute inclusions in orthopyroxene and olivine. Colourless glass (SiO_2 = 65.75, TiO_2 = 0.38, Al_2O_3 = 17.71, FeO^t = 0.83, MgO = 0.55, CaO = 0.07, Na_2O = 0.53, K_2O = 4.11 wt%) occurs interstitially along olivine neoblast boundaries (Pl. II, photo 3).

Most samples show evidence of deformation materialised by strained olivine and orthopyroxene porphyroclasts, as well as by a foliation defined by elongated grains.

Olivine neoblasts occur as subhedral to polygonal strainfree grains (locally showing typical triple junctions) sporadically associated with anhedral clinopyroxene neoblasts.

As in group II, orthopyroxene porphyroclasts exhibit abundant fluid inclusions (and melt pockets), whilst neoblasts are free of inclusions (Pl. II, photo 4). The

absence of fluid inclusions in neoblasts suggests that metasomatic processes preceded the deformation events acting on these harzburgites.

Wehrlites

Wehrlites display dominant protogranular textures; however, some of them show typical cumulus textures where poikilitic, intercumulus clinopyroxene encloses olivine crystals.

Wehrlite mineralogy comprises anhedral olivine (≤ 9 mm), light green (locally with pale purple overgrowth) clinopyroxene and minor brown to black spinel.

Most of the spinel grains are anhedral and occur interstitially; small inclusions in olivine and clinopyroxene are also present.

Dunites

Dunites display protogranular textures and, in addition to olivine (≤ 9 mm long), contain intergranular brown to black spinel (scarce as inclusions in the silicate minerals) and minor amounts (< 1 %) of interstitial, pale green clinopyroxene.

In both wehrlite and dunite, larger olivine crystals display deformation lamellae and clinopyroxenes exhibit rhonite (± spinel) exsolution lamellae and display compositional zoning (with Ti enrichment near the rim) as a result of reaction with the host basaltic/nephelinitic magmas.

MINERAL CHEMISTRY

14 representative samples of the peridotites were selected for mineral chemistry studies. The average mineral analyses for each sample are listed in tables 1 to 4. The analyses were performed on an automated JEOL JCXA733 electron microprobe, at the Centre of Geology (University of Lisbon). The analytical precision, evaluated from repeated analyses of standards, is better than ± 2%.

Olivine

Olivine is present in all the analysed samples. Olivine composition in harzburgites is homogeneous (Table 1) and within the typical range for mantle residual peridotites. Metasomatized protogranular harzburgites have slightly lower olivine Fo [Fo = $Mg/(Mg+Fe^{2+})$] contents (90-91) than the protogranular and porphyroclastic harzburgites (91-92). NiO concentrations range from 0.19 to 0.50 wt% with a minority of low values (< 0.30 wt%) that correspond to some rims of olivines in metasomatized protogranular harzburgites.

Olivines in protogranular harzburgites have low CaO contents (n.d. to 0.06 wt%) consistent with crystallisation at high pressures, whilst olivines of metasomatized and porphyroclastic harzburgites have a wider range of CaO

TABLE 1
Micropobe olivine analyses (averages)

	Protogranular			Metasomatized protogranular				Porphyr.	Wehrlites				Dunites	
Sample	**2375(1)**	**2595/x-12**	**2596/x-2**	**2592/x-4**	**2596/x-7**	**2596/x-8**	**2595/x-5**	**2595/x-8**	**2594/x-11**	**2594/x-13**	**2375(2)**	**2596/x-6**	**2375(3)**	**2594/x-3**
N.° anal.	4	8	7	2	2	7	10	9	3	2	4	6	2	5
SiO_2 (%)	41.19	41.00	41.27	40.70	41.15	41.30	41.05	41.00	39.81	39.75	40.12	40.44	40.63	40.38
TiO_2	0.00	0.01	0.00	0.00	0.01	0.01	0.01	0.01	0.01	0.02	0.01	0.01	0.02	0.01
Al_2O_3	0.00	0.01	0.00	0.01	0.02	0.01	0.00	0.01	0.02	0.01	0.02	0.02	0.01	0.11
NiO	0.37	0.40	0.42	0.29	0.23	0.37	0.32	0.39	0.23	0.23	0.21	0.24	0.35	0.24
FeO	8.38	8.41	8.50	9.39	8.52	8.90	9.47	8.26	15.54	16.60	13.67	12.61	12.17	13.62
MnO	0.12	0.13	0.17	0.13	0.14	0.06	0.17	0.13	0.26	0.30	0.25	0.18	0.16	0.18
MgO	49.77	50.31	49.71	49.10	49.96	49.58	49.57	50.30	43.47	43.43	44.74	46.69	46.83	45.52
CaO	0.03	0.02	0.03	0.14	0.05	0.10	0.13	0.16	0.17	0.11	0.38	0.23	0.05	0.18
Total	99.85	100.28	100.10	99.76	100.06	100.32	100.71	100.26	99.50	100.43	99.39	100.42	100.21	100.25
Fo (%)	91.37	91.42	91.25	90.30	91.27	90.85	90.32	91.56	83.31	82.34	85.38	86.85	87.26	85.63

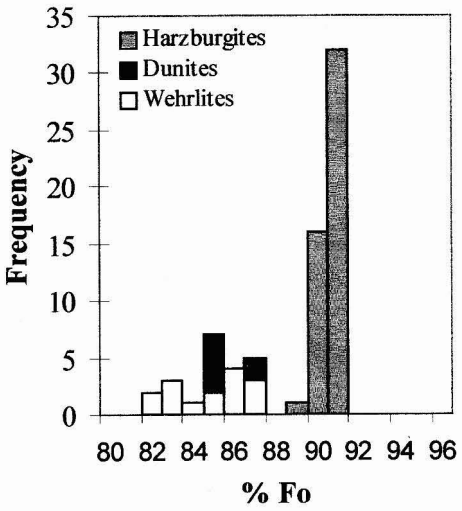

Fig. 3 – Olivine Fo histogram for the Santo Antão peridotite xenoliths.

values (0.05 to 0.24 wt%). There is no systematic core--rim chemical zonation nor compositional difference between porphyroclasts and neoblasts.

Olivines in dunites and wehrlites have lower Fo (82-88; Fig. 3), slightly lower NiO contents (0.12--0.39 wt%), and higher CaO concentrations (0.04-0.71 wt %) than harzburgites.

Orthopyroxene

Orthopyroxene is a major constituent of the harzburgites (Table 2) but is absent from wehrlite and dunite samples. All analysed orthopyroxenes in harzburgites are enstatites ($Wo_{1-4}En_{88-92}Fs_{7-9}$). Orthopyroxene Cr_2O_3 and Al_2O_3 contents in protogranular harzburgites are relatively homogeneous (0.63-0.97 wt%, $\bar{x}$ = 0.78 wt%; 2.12-3.43 wt%, $\bar{x}$ = 2.55 wt%), and generally more variable in metasomatized (0.43-0.98 wt%, $\bar{x}$ = 0.62 wt%; 0.59-2.35 wt%, $\bar{x}$ = 1.17 wt%) and porphyroclastic harzburgites (0.21-1.00 wt%, $\bar{x}$ = 0.49 wt%; 0.34-1.13 wt%, $\bar{x}$ = 0.75 wt%); neoblasts and deformed crystals show lower Al_2O_3 values.

Orthopyroxene Al_2O_3 values correlate negatively with Cr# [Cr# = $100Cr/(Cr+Al+Fe^{3+})$] in coexisting spinel (Fig. 4), as expected for residual peridotites (DICK & FISHER, 1984).

TABLE 2
Micropobe orthopyroxene analyses (averages)

	Protogranular			Metasomatized protogranular				Porphyr.	
Sample	**2375(1)**	**2596/x-2**	**2595/x-12**	**2595/x-5**	**2596/x-7**	**2596/x-8**	**2592/x-4**	**2595/x-8**	
N.° anal.	8	6	20	9	2	4	5	6P	8N
SiO_2	55.03	55.63	55.90	57.65	56.50	57.47	56.19	57.91	57.06
TiO_2	0.03	0.02	0.01	0.10	0.01	0.13	0.03	0.04	0.04
Al_2O_3	3.05	2.52	2.39	0.66	1.88	1.01	1.94	0.78	0.65
Cr_2O_3	0.76	0.76	0.80	0.48	0.69	0.68	0.80	0.46	0.52
Fe_2O_3	1.78	0.58	1.05	0.30	0.11	0.15	1.07	0.04	0.87
FeO	4.24	5.02	4.73	5.73	5.42	5.80	4.53	5.16	4.33
MnO	0.13	0.12	0.13	0.16	0.13	0.13	0.13	0.12	0.12
MgO	33.83	33.56	33.74	34.04	33.54	33.43	33.63	34.37	34.72
CaO	0.84	1.12	1.32	1.19	0.92	1.27	1.60	1.20	0.98
Na_2O	0.02	0.02	0.02	0.12	0.09	0.10	0.08	0.12	0.11
K_2O	0.01	0.00	0.00	0.01	0.01	0.00	0.00	0.01	0.00
Total	99.70	99.35	100.08	100.43	99.28	100.16	99.99	100.21	99.41
WO	1.60	2.15	2.51	2.22	1.76	2.41	3.02	2.26	1.84
EN	89.54	89.39	88.93	88.75	89.77	88.58	88.64	89.92	90.50
FS	8.86	8.46	8.57	9.02	8.47	9.01	8.33	7.82	7.66
Mg#	0.93	0.92	0.93	0.91	0.92	0.91	0.93	0.92	0.93

P – Porphyroclasts; N – Neoblasts.

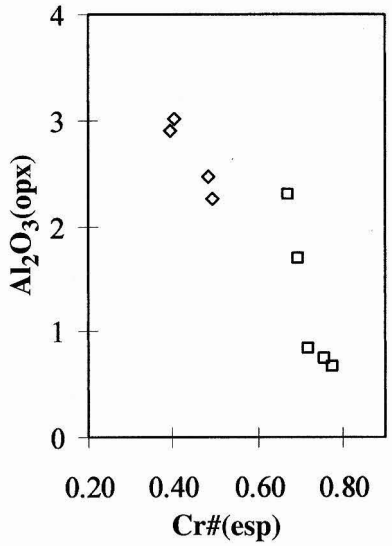

Fig. 4 – Al_2O_3 wt% (opx) *vs.* Cr# (sp) correlation in Santo Antão protogranular (*diamonds*) and metasomatised and porphyroclastic (*squares*) harzburgite xenoliths.

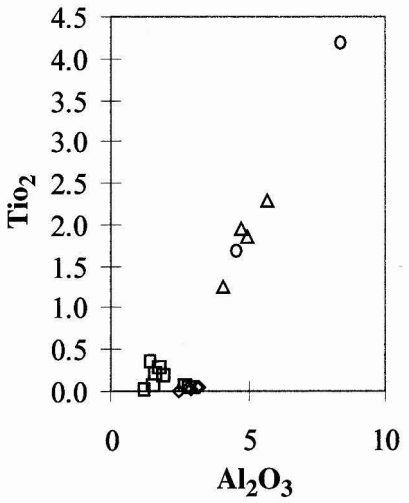

Fig. 5 – TiO_2 *vs.* Al_2O_3 (wt%) in clinopyroxenes (sample averages) from Santo Antão peridotite xenoliths. Symbols as in Fig. 6.

Clinopyroxene

Clinopyroxenes are present in all analysed samples (see Table 3 for average analyses). In harzburgites they are Cr-diopsides (Cr a.f.u. > 0.01: MORIMOTO *et al.* 1988; $Wo_{42-49}En_{59-47}Fs_{6-3}$) with Mg# = 0.90-0.97 [Mg# = Mg/(Mg+Fe^{2+})] and Cr_2O_3 varying from 0.76 to 2.70 wt%. Clinopyroxenes in protogranular harzburgites are low in TiO_2 (< 0.08 wt%) and Al_2O_3 (3-4 wt%) as typical for clinopyroxenes of residual mantle origin (JAGOUTZ *et al.*, 1979; WASS, 1979). Contrasting with cluster clinopyroxenes, the majority of metasomatic diopsides and neoblasts from metasomatized and porphyroclastic harzburgites have even lower Al_2O_3 (< 2.5 wt %) and higher TiO_2 contents (average 0.26 and 0.19 wt%, respectively; Fig. 5). Furthermore, clinopyroxenes from metasomatized and porphyroclastic harzburgites have lower Mg values (Mg# = 0.90-0.94) and display significant Na_2O enrichment (0.65-1.16 wt%) when compared to protogranular harzburgite clinopyroxenes (Mg# = 0.92-0.99; Na_2O = 0.06-0.43 wt%).

All the analysed harzburgite clinopyroxenes have $Al^{VI}/Al^{IV} > 0.25$ (Fig. 6) suggesting high pressure crystallisation (WASS, 1979).

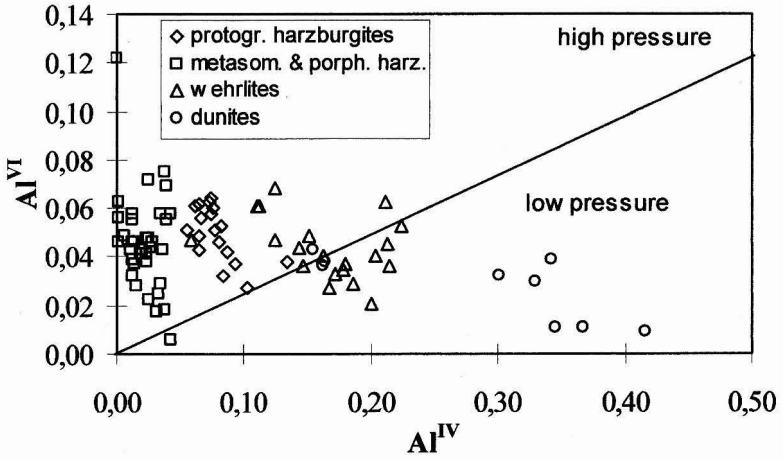

Fig. 6 – Al^{VI} *vs.* Al^{IV} (afu) of clinopyroxenes from Santo Antão peridotite xenoliths.

TABLE 3
Micropobe clinopyroxene analyses (averages)

	Protogranular					Metasomatized protogranular						Porphyr.	Wehrlites				Dunites	
Sample	**2375(1)**		**2595/x-12**		**2596/x-2**	**2592/x-4**		**2595/x-5**	**2596/x-7**	**2596/x-8**		**2595/x-8**	**2375(2)**	**2594/x-11**	**2594/x-13**	**2596/x-6**	**2375(3)**	**2594/x-3**
N° anal.	**4CLT**	**5**	**2CLT**	**6**	**1CLT**	**7**	**2**	**13**	**2CLT**	**3**	**1CLT**	**6N**	**6**	**5**	**3**	**6**	**6**	**3**
SiO_2 (%)	52.28	52.76	53.78	52.54	53.14	54.30	54.73	54.32	54.70	54.34	54.47	53.90	50.57	49.10	47.99	49.58	43.59	49.58
TiO_2	0.05	0.06	0.01	0.02	0.06	0.22	0.07	0.37	0.02	0.29	0.07	0.19	1.25	1.95	2.29	1.86	4.20	1.67
Al_2O_3	3.24	3.11	2.52	2.89	2.83	1.57	1.53	1.38	1.18	1.75	2.67	1.93	4.06	4.76	5.70	4.97	8.36	4.56
Cr_2O_3	1.16	1.08	1.28	1.19	1.08	1.32	1.64	1.98	1.12	1.97	1.24	1.87	0.92	0.78	0.69	1.15	0.46	1.01
Fe_2O_3	0.97	0.09	0.00	0.66	0.00	0.12	0.00	0.13	0.07	0.00	0.00	0.01	1.28	1.61	2.05	1.34	3.84	1.49
FeO	1.55	2.32	2.12	1.94	2.17	3.04	2.77	2.85	2.31	2.83	2.62	2.61	3.12	3.78	3.44	2.95	2.41	2.86
MnO	0.05	0.09	0.09	0.08	0.08	0.10	0.07	0.11	0.08	0.09	0.06	0.06	0.06	0.08	0.10	0.07	0.06	0.03
MgO	16.95	16.43	17.51	17.88	17.29	17.95	18.14	17.29	16.86	17.48	17.04	17.17	14.29	13.84	13.25	14.43	11.93	14.33
CaO	22.70	23.21	23.33	22.28	22.97	20.28	20.29	19.94	22.11	19.97	21.60	19.93	22.79	23.11	23.31	22.62	23.41	23.06
Na_2O	0.37	0.36	0.09	0.08	0.12	0.74	0.74	1.05	0.97	1.10	0.83	1.10	0.81	0.50	0.53	0.70	0.47	0.61
K_2O	0.00	0.01	0.01	0.01	0.01	0.01	0.01	0.02	0.01	0.00	0.00	0.01	0.01	0.00	0.00	0.01	0.00	0.01
Total	99.31	99.52	100.72	99.55	99.75	99.65	99.97	99.43	99.41	99.82	100.60	98.77	99.15	99.52	99.35	99.67	98.72	99.21
WO	47.08	48.33	47.21	45.29	47.08	42.44	42.50	42.95	46.55	42.87	45.56	43.40	49.47	49.68	50.71	49.18	52.45	49.80
EN	48.92	47.62	49.29	50.57	49.31	52.25	52.86	51.87	49.38	52.20	50.01	52.01	43.16	41.40	40.12	43.64	37.17	43.07
FS	4.00	4.04	3.48	4.13	3.60	5.30	4.62	5.17	4.06	4.91	4.43	4.57	7.35	8.91	9.15	7.17	10.38	7.12
Mg#	0.95	0.93	0.94	0.94	0.93	0.91	0.92	0.92	0.93	0.92	0.92	0.92	0.89	0.87	0.87	0.90	0.90	0.90

CLT – Cpx in cluster associations; N – Neoblasts

TABLE 4

Micropobe spinel analyses (averages)

	Protogranular			Metasomatized protogranular					Porphyr.	Wehrlites				Dunites	
Sample	**2375(1)**	**2595/x-12**	**2596/x-2**	**2592/x4**	**2595/x5**	**2596/x7**	**2596/x8**		**2595/x8**	**2375(2)**		**2594/x11**	**2594/x13**	**2596/x6**	**2375(3)**	**2594/x3**
N° anal.	**4**	**2**	**8**	**2**	**3**	**2CLT**	**3CLT**	**4**	**5**	**1core**	**1rim**	**4**	**4**	**7**	**3**	**2**
Al_2O_3	31.93	27.33	28.15	13.01	7.29	17.52	14.79	9.83	9.67	9.36	6.29	10.24	8.25	7.56	11.95	17.75	14.65
TiO_2	0.05	0.01	0.03	0.02	1.40	2.38	0.04	0.47	1.63	0.43	7.01	14.51	6.66	8.54	12.29	1.13	2.89	6.25
Cr_2O_3	34.06	41.70	41.36	38.87	49.98	55.60	46.58	51.91	53.04	57.03	24.41	5.76	23.60	13.75	7.45	52.55	32.37	23.90
V_2O_3	0.18	0.15	0.16	0.15	0.23	0.26	0.18	0.28	0.26	0.26	0.25	0.35	0.24	0.30	0.33	0.27	0.19	0.27
Fe_2O_3	4.73	1.94	1.06	3.56	5.43	4.87	7.10	4.20	5.10	4.51	24.06	31.57	24.42	32.72	31.47	4.71	15.03	21.00
FeO	13.14	14.54	14.58	13.74	16.26	17.08	12.44	12.46	15.61	14.31	26.31	32.60	24.54	28.66	31.38	14.26	19.31	23.59
MnO	0.19	0.22	0.22	0.22	0.28	0.31	0.25	0.25	0.29	0.30	0.43	0.45	0.37	0.31	0.34	0.27	0.28	0.29
MgO	15.47	14.12	14.14	14.57	11.96	11.57	14.04	14.09	12.02	12.39	8.38	8.17	9.27	7.61	7.60	12.91	11.37	10.41
Total	99.74	100.00	99.69	99.31	98.52	99.36	98.13	98.45	97.76	98.89	100.20	99.70	99.34	100.13	98.44	98.06	99.20	100.35
Mg#	0.68	0.63	0.63	0.65	0.57	0.55	0.67	0.67	0.58	0.61	0.36	0.31	0.40	0.32	0.31	0.62	0.51	0.44
Cr#	0.40	0.49	0.49	0.46	0.67	0.78	0.59	0.67	0.73	0.75	0.40	0.13	0.38	0.24	0.15	0.70	0.44	0.36

CLT – Sp in cluster associations

Cr-diopsides ($Wo_{48-51}En_{45-40}Fs_{7-9}$; Cr_2O_3 = 0.63--1.48 wt%; Na_2O = 0.45-0.93 wt%) from wherlites are poorer in Mg (Mg# = 0.87-0.92), but richer in TiO_2 (0.61-2.53 wt%) and Al_2O_3 (2.44-6.37 wt%) than the harzburgite clinopyroxenes. Dunite clinopyroxenes ($Wo_{50-53}En_{43-37}Fs_{7-10}$; Mg# = 0.85–0.94; Cr_2O_3 = 0.30--1.09 wt %; Na_2O = 0.44-0.65 wt%) are similar to those in wehrlites but reach higher TiO_2 (1.60-4.90 wt%) and Al_2O_3 (4.50-9.49 wt%) contents; $Al^{VI}/Al^{IV} < 0.25$ suggests low pressure crystallisation conditions (Fig. 6).

Spinel

Spinel is present in all the analysed samples mostly as a minor constituent (Table 4).

Harzburgite spinels are $(Mg,Fe)Al_2O_4$-$(Mg,Fe)Cr_2O_4$ solid solutions, remarkably homogeneous for each sample and even for the three textural types.

Chromiferous spinels ($Al > Cr$, $Mg > Fe^{2+}$) are dominant in protogranular harzburgites, whereas all spinels, analysed in metasomatized protogranular and porphyroclastic harzburgites, are magnesiochromites ($Cr > Al$, $Mg > Fe^{2+}$).

Protogranular harzburgite spinels have lower Cr# (0.38-0.50) and TiO_2 (< 0.06 wt%) than the metasomatized (Cr# = 0.53-0.79; TiO_2 = 1.35-2.38 wt%) and porphyroclastic (Cr# = 0.75-0.76; TiO_2 = 0.40-0.43 wt%) harzburgite spinels. In these harzburgites, spinels forming vermicular clusters also have low titanium (TiO_2 = 0.03-0.56 wt%). Fig. 7 shows that all protogranular

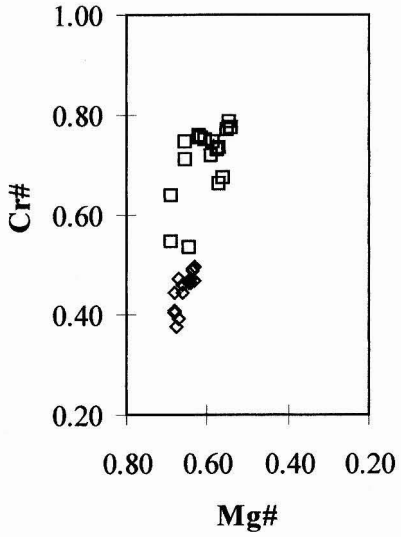

Fig. 7 – Cr# *vs.* Mg# in spinels from Santo Antão harzburgite xenoliths. Symbols as in Fig. 6.

harzburgite spinels fall within the field defined for abyssal peridotites and basalts (DICK & BULLEN, 1984; DICK & FISHER, 1984) whereas most of the metasomatized protogranular and porphyroclastic harzburgite spinels fall above that field.

Wehrlite spinels are more heterogeneous than those in harzburgites. Despite the observed chemical variation (Mg# = 0.27-0.58; Cr# = 0.13-0.42; TiO_2 = 1.13-14.85 wt%) most wehrlite spinels correspond to Al, Cr, Mg – rich Ti-magnetites (Fe^{3+} > Al, Cr), indicating extensive solid solution among ulvospinel, magnetite, chromite and spinel (s.s.) endmembers. However, with the exception of chromite to magnetite, core to rim, chemical zonation in sample 2375(2), the remaining spinels are relatively homogeneous within each sample.

Spinels in dunites are chromites and magnesiochromites (Mg# = 0.44–0.53; Cr# = 0.36-0.44; TiO_2 = 2.87-6.30 wt%).

GEOTHERMOMETRY AND OXYGEN GEOBAROMETRY

Equilibration temperatures for Santo Antão spinel peridotites have been estimated using different thermometric methods (see Table 5 for results).

TABLE 5
Geothermometric estimates for peridotite xenoliths from Santo Antão

SAMPLES	METHODS									
	Opx - Cpx					Opx - Ca	Ol - Sp			
	W&B	**WEL**	**B&M**	**KRET**	**B&K1**	**B&K2**	**FAB**	**ROED**	**O&W**	**BALH**
HARZBURGITES										
Protogranular										
2375(1)	1004	883	806	885	829	945				
	1151	1052	1080	1060	1030	879	784	802	755	883
2595/x-12	1068	964	924	978	1009	1080				
	1083	967	902	958	937	1137	794	774	758	837
2596/x-2	1089	977	923	971	954	1000	806	803	781	899
	1083	977	922	971	948	985				
Metasom. Prot.										
2592/x-4	1197	1104	1097	1132	1136	1137	881	833	923	990
2596/x-8	1156	1071	1074	1136	1109	1074	942	917	1014	1075
							975	982	1040	1124
	1139	1048	1045	1113	1070	1074				
2595/x-5	1164	1085	1088	1153	1117	1086	923	872	996	1046
	1158	1070	1085	1141	1118	1048				
Porphyroclastic										
2595/x-8	1105	998	982	1045	1018	1074	910	861	957	1006
	1133	1025	1035	1097	1081	889	914	867	959	1033
DUNITES										
2375(3)							847	831	932	996
2594/x-3							832	814	987	1032
WHERLITES										
2375(2)							829	793	1015	1058
2594/x-11							748	660	975	1001
2594/x-13							608	500	939	956
							672	558	981	975
2596/x-6							845	881	951	1019
							885	915	971	1053

W&B – WOOD & BANNO (1973); WEL – WELLS (1977); B&M – BERTRAND & MERCIER (1985); KRET – KRETZ (1982); B&K1 and B&K2 – BREY & KOHLER (1990); FAB – FABRIÈS (1979); ROED – ROEDER *et al.* (1979); O&W – O'NEILL & WALL (1987); BALH – BALLHAUS *et al.* (1991).

The two-pyroxene geothermometric methods (WELLS, 1977; KRETZ, 1982; BREY & KOHLER, 1990) show good agreement for most samples, whereas the olivine-spinel geothermometers (FABRIÈS, 1979; ROEDER *et al.*, 1979; O'NEILL & WALL, 1987; BALLHAUS *et al.*, 1991) indicate lower temperatures. We will give preference to the most widely used two-pyroxene method of WELLS (1977) and the Ol-Sp geothermometers of O'NEILL & WALL (1987) and BALLHAUS *et al.* (1991).

The average two-pyroxene (WELLS, 1977) temperature determined from protogranular harzburgite "primary" minerals is 970 ± 80 °C. This is about 80 to 200 °C higher than olivine-spinel temperatures (BALLHAUS *et al.*, 1991; O'NEILL & WALL, 1987) determined in the same samples (890 ± 10 °C; 770 ± 15 °C), supporting high Fe⇔Mg interdiffusion rates in spinel that made them prone to resetting during slow cooling. Geothermometric estimates on neoblasts (T_{WELLS} = 1050 ± 50 °C; $T_{O'NEILL\ \&\ WALL}$ = 980 ± 60 °C; $T_{BALLHAUS\ et\ al.}$ = 1060 ± 70 °C) indicate higher temperatures, suggesting that harzburgites underwent complex thermal evolution. Indeed, calculated temperatures range from ~750 °C (corresponding to long term equilibria during cooling from magmatic temperatures, deformation and metasomatic neoblast re-crystallization) to ~ 1100 °C.

In contrast, the temperature estimates for wehrlites and dunites ($T_{O'NEILL\ \&\ WALL}$ = 970 ± 40 °C; $T_{BALLHAUS\ et\ al.}$ = 1000 ± 50 °C) are much more homogeneous, suggesting a simpler thermal history for these xenolith types.

Given the geothermometric data above, fO_2 values attending harzburgite equilibria were estimated from NELL & WOOD (1991) calibration of the olivine-orthopyroxene-spinel oxygen sensor (application of the BALLHAUS *et al.* (1991) model to Santo Antão spinels yields essentially the same fO_2 results). According to that oxygen geobarometer, most Santo Antão harzburgite xenoliths are 0.7 to 1.9 log units more oxidized than the FMQ buffer (Fig. 8), well within the fO_2 range reported for lithospheric xenoliths sampled by ocean island basaltic magmas elsewhere (BALLHAUS, 1993). Given its lower fO_2, protogranular harzburgite 2595/x-12 (Fig. 8) probably represents xenolithic material that was the least affected (or even unaffected) by metasomatic fluids.

CONCLUDING REMARKS

Ultramafic xenoliths occurring in alkalic lavas on Santo Antão Island are divided into wehrlite/dunite and harzburgite suites.

On the basis of petrography and mineral chemistry wehrlite/dunite xenoliths (poikilitic textures; Fo < 89%; high $TiO_{2(cpx\ and\ sp)}$) are interpreted as crystal cumulates (probably) derived from alkalic magmas, similar to those that give rise to Santo Antão Island.

The harzburgite suite xenoliths (primary crystals: Fo > 90%; $TiO_{2(cpx\ and\ sp)}$ < 0.08 wt%; inverse correlation of $Al_2O_{3(opx)}$ *vs.* $Cr\#_{(sp)}$) originated in the mantle and are interpreted as representing depleted oceanic lithosphere that was variously modified by metasomatic and tectonic processes. Protogranular harzburgites (group I) are fragments of residual mantle, unaffected or slightly affected by metasomatic and deformation processes; metasomatized protogranular harzburgites (group II) correspond to the reaction of residual mantle with metasomatic fluids (apparently a Ti-rich silicate melt) as suggested by the abundant fluid inclusions and melt pockets in orthopyroxene, growing of Na-rich clinopyroxene at the expense of orthopyroxene and the Ti-enriched character of clinopyroxene and spinel; porphyroclastic harzburgites (group III) clearly reveal a deformation episode. Neoblasts void of fluid inclusions demonstrate that the metasomatic episode preceded deformation.

Following traditional nomenclature, the harzburgite suite xenoliths belong to Group I and the wehrlite/dunite suite xenoliths to Group II of FREY & PRINZ (1978).

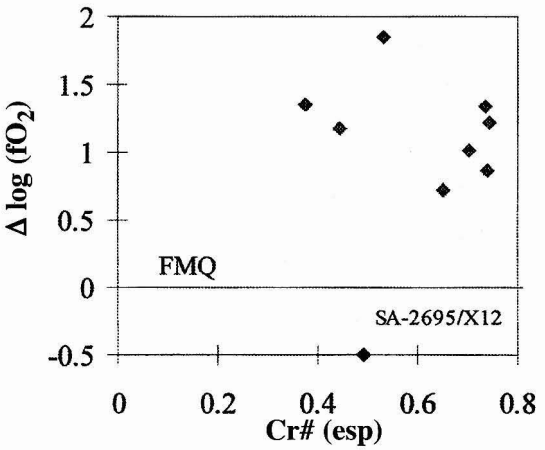

Fig. 8 – Δ log (fO_2) *vs.* Cr# of spinel from Santo Antão harzburgite xenoliths. Oxygen fugacity calculation using the NELL & WOOD (1991) method.

The occurrence of wehrlite/dunite cumulate xenoliths indicates that magma reservoir(s) existed at depth beneath Santo Antão Island prior to the eruption of the xenolith-bearing lavas. Thus, in order to avoid removal from ascending host magmas, the harzburgite xenoliths must have been located in the upper mantle, above these intermediate depth magma reservoir(s) (CLAGUE, 1988); this was a region of relatively high strain rate, probably near the boundary between the mantle and the overlying ocean crust.

ACKNOWLEDGEMENTS

Funding for field work was provided by IICT and ICP (now IPAD). This work was partially supported by research funds from Project POCA (POCTI-FEDER) to Centro de Geologia da FCUL.

REFERENCES

BALLHAUS, C., BERRY, R. F. & GREEN, D. H. (1991) – High pressure experimental calibration of the olivine-orthopyroxene-spinel oxygen geobarometer: implications for the oxidation state of the upper mantle. *Contrib. Mineral. Petrol.*, **107**, pp. 27-40.

BALLHAUS, C. (1993) – Redox states of lithospheric and asthenospheric upper mantle. *Contrib. Mineral. Petrol.*, **114**, pp. 331--348.

BERTRAND, P. & MERCIER, J. C. (1985) – The mutual solubility of coexisting ortho- and clinopyroxene: toward an absolute geothermometer for the natural system? *Earth Planet. Sci. Lett.*, **76**, pp. 109-122.

BREY, G. P. & KOHLER, T. (1990) – Geothermobarometry in four phase lherzolites II. New thermobarometers, and practical assessment of existing thermobarometers. *J. Petrol.*, **31** (6), pp. 1353-1378.

CLAGUE, D. A. (1988) – Petrology of ultramafic xenoliths from Loihi Seamount, Hawaii. *J. Petrol.*, **29** (6), 1161-1186.

DAVIES, G. R. & MENDES, M. H. (1991) – The petrogenesis of metasomatized sub-oceanic mantle beneath Santiago: Cape Verde Islands. *Fifth Intern. Kimberlite Conference*, Araxá, Brasil. CPRM Spec. Publ.2/91, pp. 66-68.

DE PÄEPE, P. & KLERKX, J. (1971) – Peridotite nodules in nephelinites from Sal (Cape Verde Islands). *Ann. Soc. Geol. Belgique*, **41**, pp. 311-316.

DICK, H. J. B. & BULLEN, T. (1984) – Chromian spinel as a petrogenetic indicator in abyssal and alpine-type peridotites and spatialy associated lavas. *Contrib. Mineral. Petrol.*, **86**, pp. 54-76.

DICK, H. J. B. & FISHER, R. L. (1984) – Mineralogical studies of the residues of mantle melting: abyssal and alpine-type peridotites. *In*: KORNPROBST, J. (ed.), Kimberlites II – *The mantle and crust-mantle relationships*. Elsevier, Amsterdam, pp. 295-308.

FABRIÈS, J. (1979) – Spinel-olivine geothermometry in peridotites from ultramafic complexes. *Contrib. Mineral. Petrol.*, **69**, pp. 329--336.

FREY, F. A. & PRINZ, M. (1978) – Ultramafic inclusions from San Carlos, Arizona: petrologic and geochemical data bearing on their petrogenesis. *Earth Planet. Sci. Lett.*, **38**, 129-176.

GERLACH, D. C., CLIFF, R. A., DAVIES, G. R., NORRY, M. & HODGSON, N. (1988) – Magma sources of the Cape Verde archipelago: isotopic and trace element constraints. *Geochim. Cosmochim. Acta*, **52** (12), pp. 2979-2992.

HARTE, B. (1977) – Rock nomenclature with particular relation to deformation and recrystallisation textures in olivine-bearing xenoliths. *J. Geol.*, **85**, pp. 279-288.

JAGOUTZ, E., PALME, H., BADDENHAUSEN, H., BLUM, K., CENDALES, M., DREIBUS, G., SPETTEL, B., LORENZ, V. & WANKE, H. (1979) – The abundances of major, minor, and trace elements in the earth's mantle as derived from primitive ultramafic nodules. *Proc. 10th Lunar Planet. Sci. Conf.*, pp. 2031-2050.

KOGARKO, L. N. & SENIN, V. G. (1993) – Physicochemical parameters of the oceanic mantle in the Cape Verde Islands. *Geochem. Intern.*, **30** (5), pp. 1-8.

KRETZ, R. (1982) – Transfer and exchange equilibria in a portion of the pyroxene quadrilateral as deduced from natural and experimental data. *Geochim. Cosmochim. Acta*, **46**, pp. 411-421.

MENDES, M. H. (1984) – *Sobre a origem dos nódulos peridotíticos de S. Nicolau (Arquipélago de Cabo Verde)*. MSc Thesis, Universidade de Aveiro, 106p.

—— (1995) – *Petrologia e geoquímica dos xenólitos peridotítico da ilha de Santiago, Arquipélago de Cabo Verde*. Thesis, IICT, Lisboa, 186p.

MENDES, M. H. & SILVA, L. C. (1983) – Preliminary note on the occurrence of peridotite nodules in Santiago (Cape Verde Islands). *Garcia de Orta, Sér. Geol.*, **6** (1-2), 175-178.

MENZIES, M. (1987) – Alkaline rocks and their inclusions: a window on the Earth's interior. *In:* FITTON, J. G. & UPTON, B. G. J. (ed.) – *Alkaline Igneous Rocks*. Geol. Soc. Sp. Publ., **30**, pp. 15-27.

MERCIER, J. C. C. & NICOLAS, A. (1975) – Textures and fabrics of upper-mantle peridotites as illustrated by xenoliths from basalts. *J. Petrol.*, **16** (2), pp. 454-487.

MORIMOTO, N., FABRIÈS, J., FERGUSON, A. K., GINZBURG, I. V., ROSS, M., SEIFERT, F. A., ZUSSMAN, J., AOKI, K. & GOTTARDI, G. (1988) – Nomenclature of pyroxenes. *Am. Mineral.*, **73**, pp. 1123--1133.

MUNHÁ, J. M., MENDES, M. H., PALÁCIOS, T., SILVA, L. C. & TORRES, P. C. (1997) – *In:* RÉFFEGA, A. *et al.* (ed.) – *A Erupção vulcânica de 1995 na ilha do Fogo*, Cabo Verde. IICT, Lisboa, pp. 171-186.

NELL, J. & WOOD, B. J. (1991) – High-temperature electrical measurements and thermodynamic properties of Fe_3O_4-$FeCr_2O_4$-$MgCr_2O_4$-$FeAl_2O_4$ spinels. *Am. Mineral.*, **76**, pp. 405-426.

O'NEILL, H. ST.C & WALL, V. J. (1987) – The olivine-orthopyroxene-spinel oxygen geobarometer, the nickel precipitation curve, and the oxygen fugacity of the Earth's upper mantle. *J. Petrol.*, **28** (6), pp. 1169-1191.

PLESNER, S., HOLM, P. M. & WILSON, J. R. (2002) – ^{40}Ar-^{39}Ar geochronology of Santo Antão, Cape Verde Islands. *J. Volcanol. Geotherm. Res.*, **120**, pp. 103-121.

ROEDER, L. P., CAMPBELL, I. H. & JAMIESON, H. E. (1979) – A re-evaluation of the olivine-spinel geothermometer. *Contrib. Mineral. Petrol.*, **68**, pp. 325-334.

RYABCHIKOV, I. D., NTAFLOS, T., KURAT, G. & KOGARKO, L. N. (1995) – Glass-bearing xenoliths from Cape Verde: evidence for a hot rising mantle jet. *Mineral. Petrol.*, **55**, pp. 217-237.

SILVA, L. C., SERRALHEIRO, A., TORRES, P. C., MADEIRA, J., MENDES, M. H. & GOMES, A. M. (in preparation) – Geologia da Ilha de Santo Antão, Cabo Verde.

STRECKEISEN, A. (1976) – To each plutonic rock its proper name. *Earth Sci. Rev.*, **12**, 1-33.

WASS, S. Y. (1979) – Multiple origins of clinopyroxenes in alkali basaltic rocks. *Lithos*, **12**, pp. 115-132.

WELLS, P. R. A. (1977) – Pyroxene thermometry in simple and complex systems. *Contrib. Mineral. Petrol.*, **62**, pp. 129-139.

WOOD, B. J. & BANNO, S. (1973) – Garnet-orthopyroxene and orthopyroxene-clinopyroxene relationships in simple and complex systems. *Contrib. Mineral. Petrol.*, **42**, 109-124.

Artigo recebido em Abril de 2004
Aceite em Maio de 2004

PLATES

PLATE I

Photo 1 – Peridotite xenoliths in nephelinitic lavas at a road section from Cova to Porto Novo.

Photo 2 – Protogranular harzburgite (Cova – Porto Novo).
ol – olivine, opx – orthopyroxene, cpx – clinopyroxene, sp – spinel.

Photo 3 – Metasomatized protogranular harzburgite (João de Arado).
Orthopyroxene (opx) melt pocket containing olivine and spinel neoblasts enclosed in glass (gl).

Photo 4 – Metasomatized protogranular harzburgite (Ribeira Grande – Ponta do Sol).
Orthopyroxene (opx) relicts rich in CO_2 fluid inclusions replaced by metasomatic clinopyroxene (cpx).

1

2
opx
cpx
ol
sp
0.8 mm

3
gl
opx
0.02 mm

4
ol
cpx
opx
0.08 mm

PLATE II

Photo 1 – Metasomatized protogranular harzburgite (João de Arado).
Olivine (ol) corroded by metasomatic clinopyroxene (cpx).

Photo 2 – Porphyroclastic harzburgite (Cova – Porto Novo).
Orthopyroxene (opx) porphyroclast in a neoblast matrix consisting of olivine and orthopyroxene. Linear aggregates of small, dark brown spinel grains are clearly shown.

Photo 3 – Porphyroclastic harzburgite (Cova – Porto Novo).
Colourless glass (gl) along olivine (ol) neoblast boundaries.

Photo 4 – Porphyroclastic harzburgite (Cova – Porto Novo).
Orthopyroxene porphyroclast rich in spinel and fluid inclusions (*left*) and olivine neoblasts free of inclusions.

2
opx
0.3 mm

4
0.02 mm

1
ol
cpx
1 mm

3
ol
gl
0.02 mm